Electronic Supplementary Material (ESI) for Journal of Materials Chemistry B.

Synthesis of Silver Nanoparticles for the Dual Delivery of Doxorubicin and Alendronate to Cancer Cells

*Farah Benyettou, Rachid Rezgui, Florent Ravaux, Talal Jaber, Katharine Blumer Mustapha Jouiad, Laurence Motte, John-Carl Olsen, Carlos Platas-Iglesias, Mazin Magzoub and Ali Trabolsi**

General methods

All reagents were purchased from a commercial supplier (Sigma-Aldrich) and used without further purification. Nanopure water (conductivity of 0.06 μS cm^{-1}), obtained from a Millipore Gradiant Elix-3/A10 system was used to prepare the sample solutions. Silver concentration was deduced from ultraviolet-visible absorption spectra recorded with an Agilent Technologies Cary 5000 Series UV-Vis-NIR spectrophotometer in water at room temperature (298 K). Solutions were examined in 1 cm spectrofluorimetric quartz cells. The experimental error of the wavelength values was estimated to be ±1 nm. Infrared spectra were recorded on an Agilent Technologies Cary 600 Series FTIR spectrometer using the ATR mode. Size and morphology of the nanoparticles were determined by scanning electron microscopy (FEI Quanta FEG 450) equipped with EDAX, to determine the elemental composition of the samples, and by transmission electron microscopy (FEI-Titan 300). Dynamic light scattering (DLS) measurements were performed on a Malvern Zetasizer NanoSeries to obtain the size and ζ-potential of the nanoparticles. DLS measurements were made on solutions of pH = 2 to 10. Thermogravimetric analyses were performed on a TA SDT Q600 device. Emission spectra were recorded in water, at room temperature using a Perkin Elmer LS55 fluorescence spectrometer. Proton and Phosphorous Nuclear magnetic resonance (^{1}H NMR) spectra were recorded at 298 K on a Bruker Advance 600 spectrometer with a working frequency of 600 MHz. Chemical shifts are reported in ppm relative to the signals corresponding to the residual non-deuterated solvent (D_2O (δ = 4.97)).

1. Synthesis

1.1. Alendronate synthesis

Alendronate (Ald, (4-amino-1-hydroxy-1-phosphonobutyl)phosphonic acid) was synthesized according to the general procedure[1] for linear aliphatic bisphosphonic acids (BPs) and characterized by ^{1}H and ^{31}P NMR. 4-aminobutyric acid (150 mmol) and phosphorous acid (150 mmol) were introduced into a three-necked round-bottom flask under inert atmosphere followed by 30 ml of methane sulfonic acid. After heating at 65 °C for 1 h, phosphorus trichloride (300 mmol) was added slowly and the reaction was allowed to proceed overnight at 65 °C. The resulting viscous yellow reaction mixture was cooled to room temperature and quenched with 500 ml of ice-cold water. The pH was adjusted to 4.3 with an aqueous NaOH solution (0.5 M), and the white precipitate obtained was collected by filtration. This solid was washed five times with a mixture of methanol/water (95:5) and freeze-dried to yield alendronate in 82% yield. ^{31}P NMR (80.9 MHz, H_3PO_4/D_2O): 18.47. ^{1}H NMR (500 MHz, D_2O): 3.046 (m, 2H), 2.017 (m, 4H). I.R.: 1640, 1540, 1172, 1052 cm^{-1}

1.2. Synthesis of Ald@AgNPs

An aqueous solution of silver nitrate (0.85 M, 1 mL) was added to an aqueous solution of alendronate (0.15 M, 1 mL) and transferred to a 10 mL vessel with a crimp cap. The mixture was heated by microwave irradiation of 2.45 GHz in a microwave reactor (CEM Discovery, CEM Inc. USA). The power was modulated in order to reach a temperature of 70 °C in one minute. The temperature was maintained for 15 minutes. The maximum power applied was 300 W. Stirring was initiated at 70 °C during the heating cycle. A yellowish solution was obtained confirming the presence of silver NPs. The solution was dialyzed for several days to remove free alendronate.

No AgNPs formed during a control experiment in which alendronate was replaced by its diphenyl ester.

1.3. Dye and drug conjugation to Ald@AgNPs

1.3.1. Rhodamine conjugation to Ald@AgNPs: RhB-Ald@AgNPs

An aqueous solution of Ald@AgNPs of 11 nm diameter (1 mL, [Ag] = 8.10^{-5} M, $n_{ald} = 1.10^{-8}$ mol) was added to an aqueous mixture containing Rhodamine B (3.10^{-8} mol), 1-ethyl-3-(3-dimethylaminopropyl)carbodiimide (EDC, 0.15 mg, 10^{-6} mol) and *N*-hydroxysuccinimide (NHS, 0.2 mg, 10^{-6} mol). The mixture was stirred for 24 hours at room temperature. The

resulting hybrid fluorescent nanoparticles formed a flocculate, which was dialyzed for 2 days. The efficiency of the conjugation was qualitatively evaluated by fluorescence spectroscopy.

1.3.2. Doxorubicine conjugation to Ald@AgNPs: Dox-Ald@AgNPs

An aqueous solution of Ald@AgNPs of 11 nm diameter (1 mL, [Ag] = 8.10^{-5} M, n_{ald} = 1.10^{-8} mol) was added to an aqueous mixture containing Dox (3.10^{-8} mol), EDC (0.15 mg, 10^{-6} mol) and NHS (0.2 mg, 10^{-6} mol). The mixture was stirred for 24 hours at room temperature. The resulting hybrid fluorescent nanoparticles formed a flocculate, which was dialyzed for 2 days. The solid, designated Dox-Ald@AgNPs, was collected by filtration. The efficiency of the conjugation was qualitatively evaluated by fluorescence spectroscopy.

1.3.3. Doxorubicine conjugation to Alendronate

We mixed together Dox (1 eq.) and Ald (0.9 eq.) in water in presence of coupling agents (EDC/NHS, 10 eq.) for 24 hours at room temperature. The water was evaporated and the solid was washed several times with acetone in order to remove un-reactant compounds.

The FTIR spectrum of the red solid was not simply the sum of the separate components, which strongly suggested an interaction between Dox and Alendronate. Free doxorubicin displays a peak at 1729 cm^{-1} corresponding to the carbonyl bond. After conjugation, this peak disappeared and a strong peak at 1706 cm^{-1} rose corresponding to the formation of the imine bond. It is worth noting that the amine vibration band of Dox at 1610 cm^{-1} remains unchanged after the conjugation and as a consequence is not involved in the bond between Alendronate and Dox, while the amine of Alendronate at 1641 cm^{-1} disappeared completely due to the imine band formation.

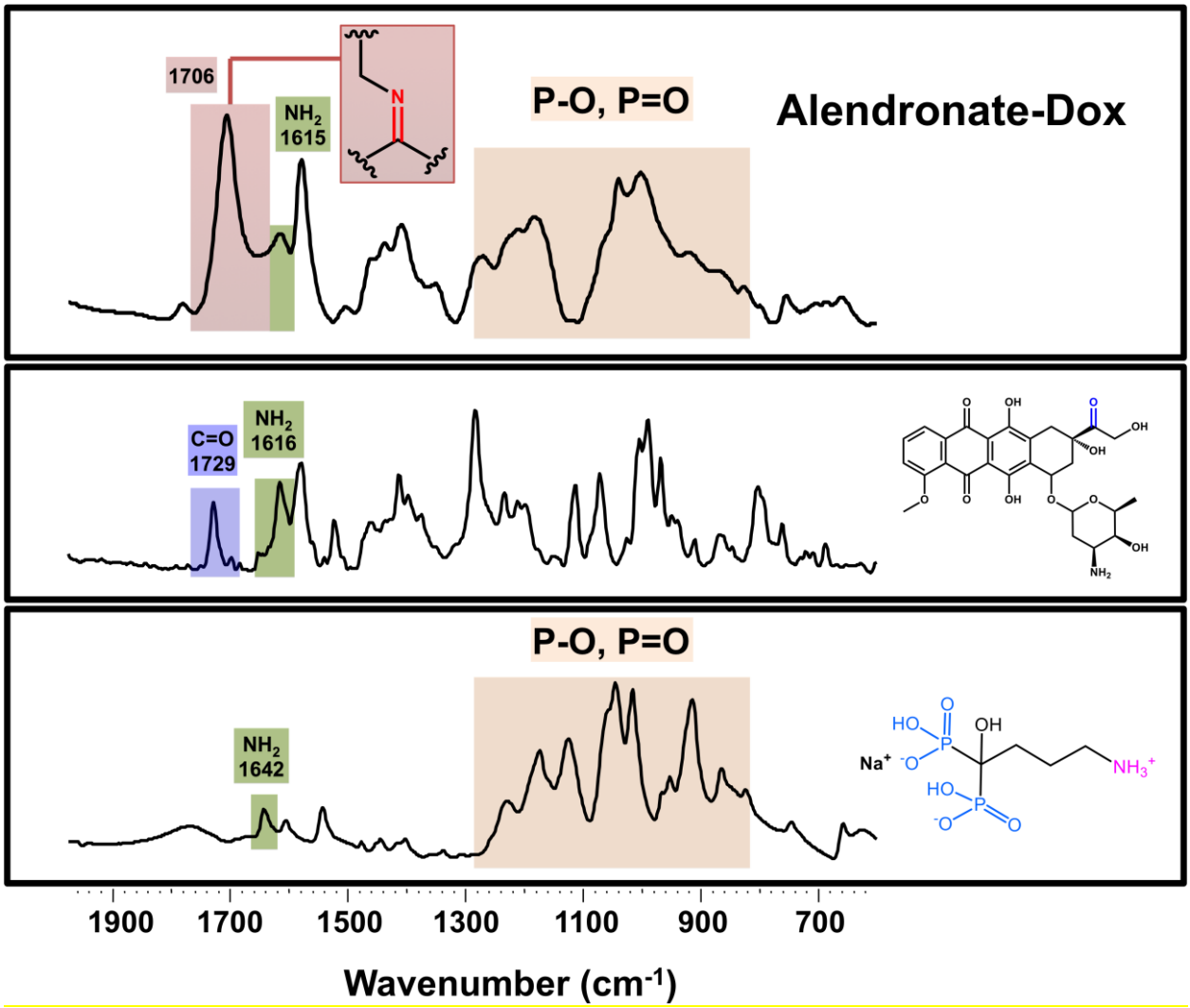

Figure S1. Comparison of FTIR spectra of Alendronate coupled to Dox, free Dox and free Ald.

2. Characterization of Ald@AgNPs

2.1. Scanning electron microscope (SEM)

The size and morphology of the Ald@AgNPs were studied using a FEI Quanta FEG scanning electron microscope 450 (SEM) capable of energy-dispersive X-ray spectroscopy (EDX) for elemental analysis. A thin film was prepared by drop-coating a diluted solution of NPs onto a silicon surface. The thin film was allowed to stand overnight at room temperature. The SEM images were recorded at 10.00 kV and 20.00 kV.

2.2. Elemental analysis (EDAX)

EDX analysis of Ald@AgNP powder (Fig. S2) shows an elemental composition of C, O, P, N, and Ag. This composition and particularly the presence of phosphorous atoms supports the presence of alendronate molecules. The silicon peak is due to the silicon surface on which the NPs were deposited.

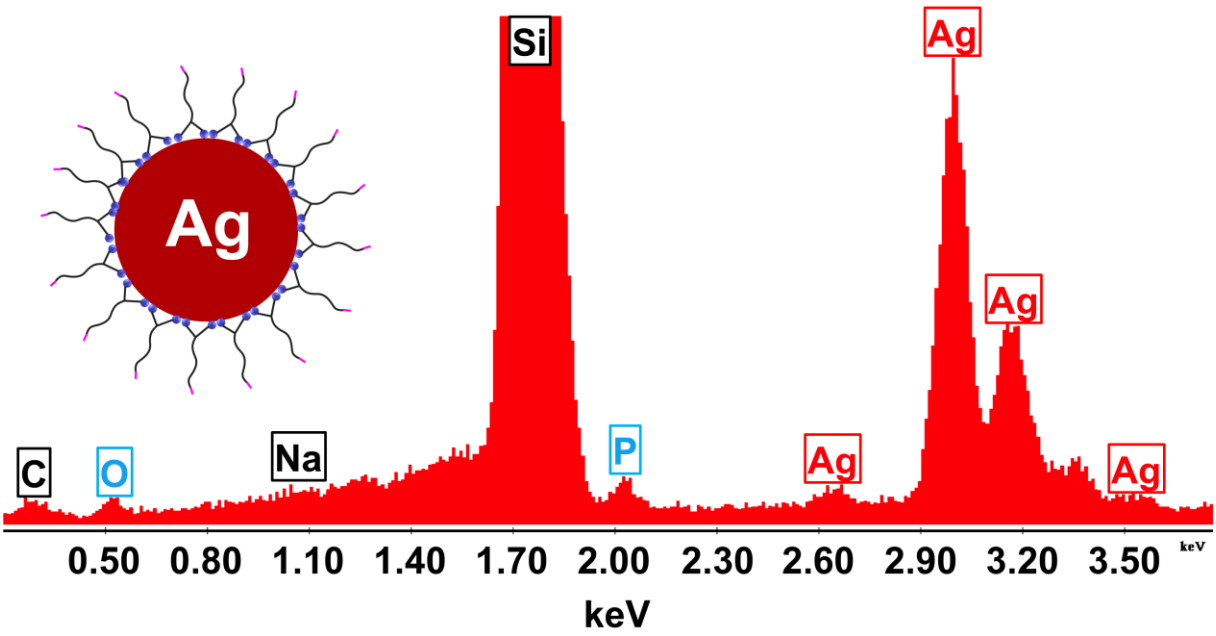

Figure S2. The EDX pattern of Ald@AgNPs.

2.3. Transmission electron microscopy (TEM)

Size and morphology of the nanoparticles were confirmed with a FEI-Titan 300 microscope operating at 200 kV. Samples were prepared on a carbon-coated copper grid. A drop of NP solution ([Ag] = 1.0×10^{-5} M) was spotted on the grid and allowed to dry overnight. The particle size distribution was determined using a standard methodology.[2] In all cases the nanoparticles had spherical shape, and their TEM size measurements were consistent with those of SEM.

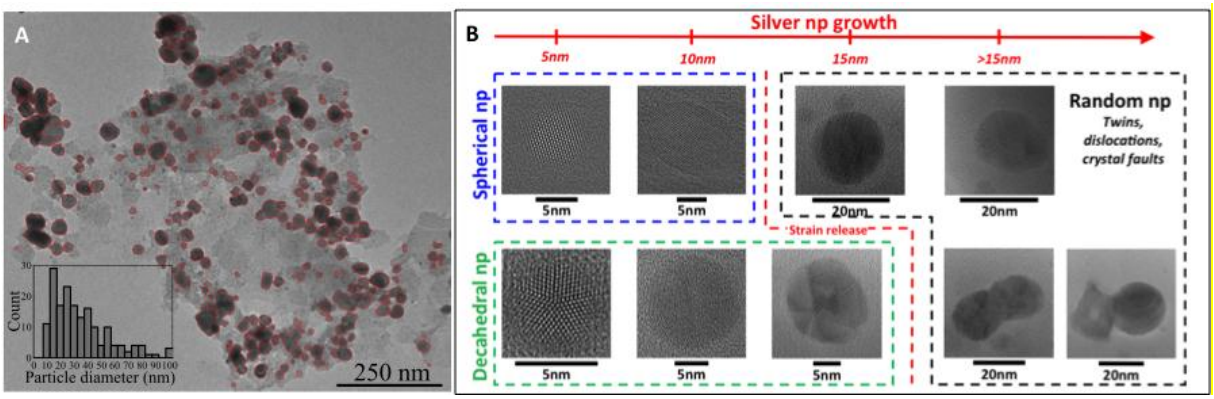

Figure S3. A) TEM micrograph of Ald@AgNPs. Inset: size distribution showing an average size of 12 nm in diameter. B) Shape of the Ald@AgNPs as function of the NP size.

2.4. UV-Visible Spectroscopy

The synthesized Ald@AgNPs were characterized by UV–Vis spectroscopy. The measurement was carried out by using an Agilent Technologies Cary 5000 Series UV-Vis-NIR Spectrophotometer having operational range of wavelength between 200 nm and 800 nm. UV–vis spectroscopy was used to authenticate the formation and stability of silver and gold NPs in aqueous solution. The absorption spectrum exhibited a strong broad peak which was assigned to a surface plasmon resonance of the as-synthesized nanoparticles.

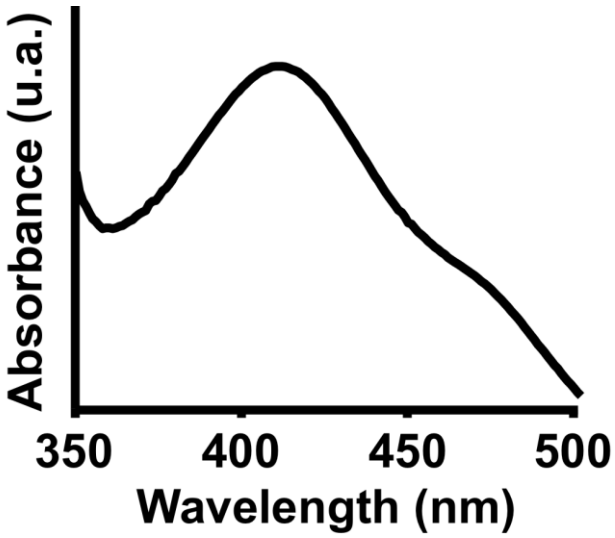

Figure S4. Absorption spectrum of Ald@AgNPs samples synthesized by MW irradiation and with [Ag] = 0.85 M, [Ald] = 0.15 M, t = 5 min and temperature of 70 C°. The peak at 470 nm represents small positively charged silver clusters, and the peak at 411 nm represents the larger AgNPs. The spectrum supports a stepwise mechanism of AgNP formation.

2.5. ^{31}P NMR spectroscopy

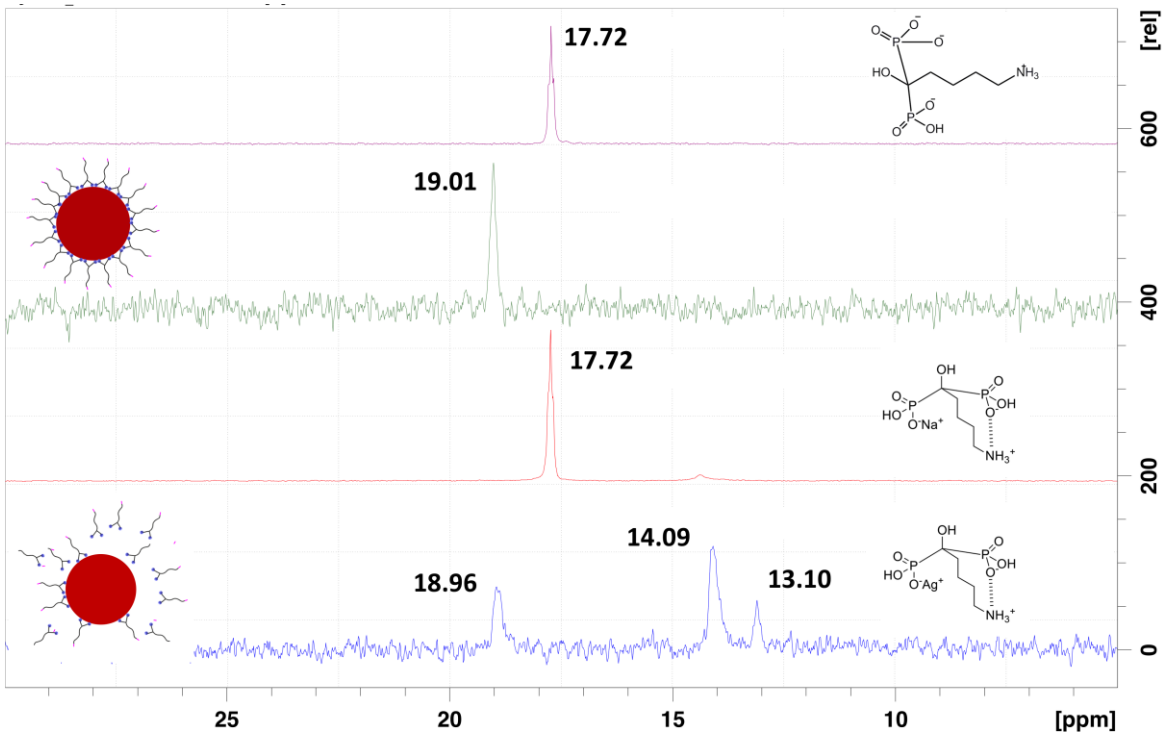

Figure S5. ^{31}P NMR (600 MHz) spectra of A) Alendronate (pH=7.4), B) Ald@AgNP(pH=7.4), C) Alendronate (pH=5.4), and D) Ald@AgNP (pH=5.4) .

2.6. Fluorescence emission spectroscopy

AgNPs have characteristic fluorescence emission properties.[3] Ald@AgNPs excited at 405 nm in water at pH 7 showed an emission maximum centered at 532 nm (Figures S6). Fluorescence is the result of metal-ligand charge-transfer interactions between silver and Ald in the Ald@AgNPs

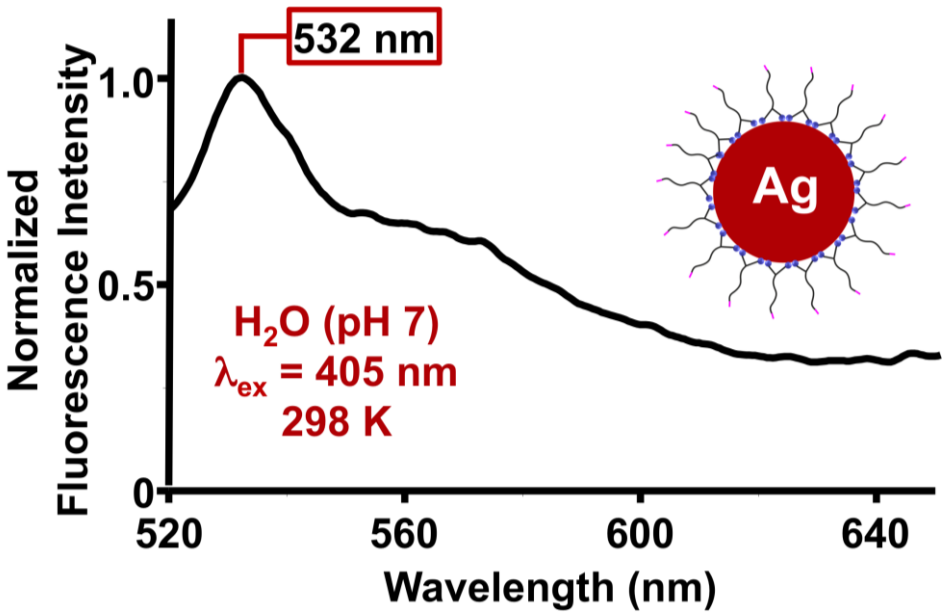

Figure S6. Fluorescence emission spectrum of Ald@AgNPs in H_2O at pH 7, 298 K and with λ_{ex} = 405 nm.

2.7. Dynamic light scattering (DLS) characterization

To determine the suitability of the nanoparticles for biomedical applications, particle size was measured and ζ-potential was calculated as a function of pH using a Zetasizer Nano-ZS spectrometer (Malvern Instruments). All samples were analyzed at room temperature in water with diluted solutions ([Ag] = 1×10^{-3} M).

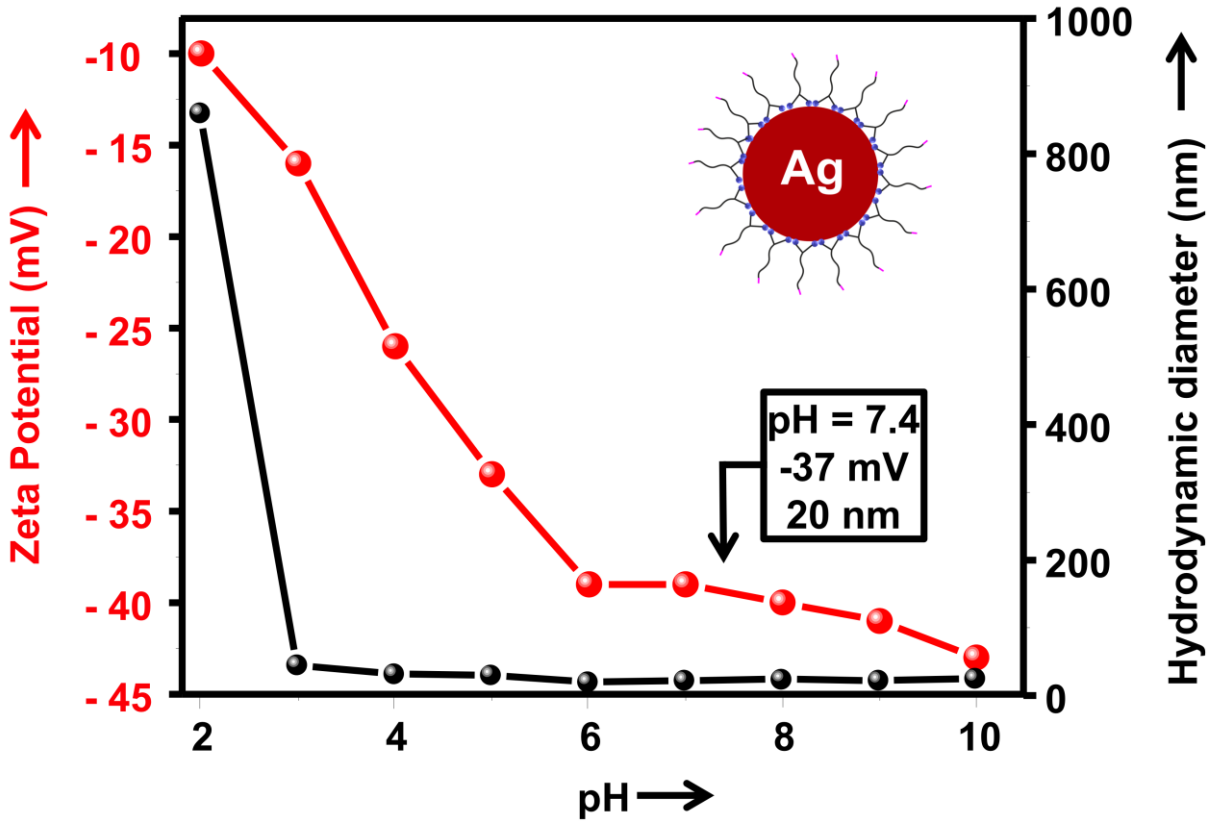

Figure S7. ζ-potential (red curve) and hydrodynamic diameter (black curve) of Ald@AgNPs as function of the pH. The boxed numbers represents the values of ζ-potential and diameter of Ald@AgNPs at physiological pH = 7.4.

2.8. Thermogravimetric analysis (TGA)

The weight percentage of alendronate on the surface of Ald@AgNPs was determined by TGA. Solid samples (10 mg) under $N_{2(g)}$ flux were characterized with a SDT Q600 TA Instruments analyzer at a heating rate of 5 °C/min over a temperature range of 35–700 °C. Figure S8 shows the weight losses of Ald@AgNPs as a function of temperature. (Inset: TGA of free alendronate).

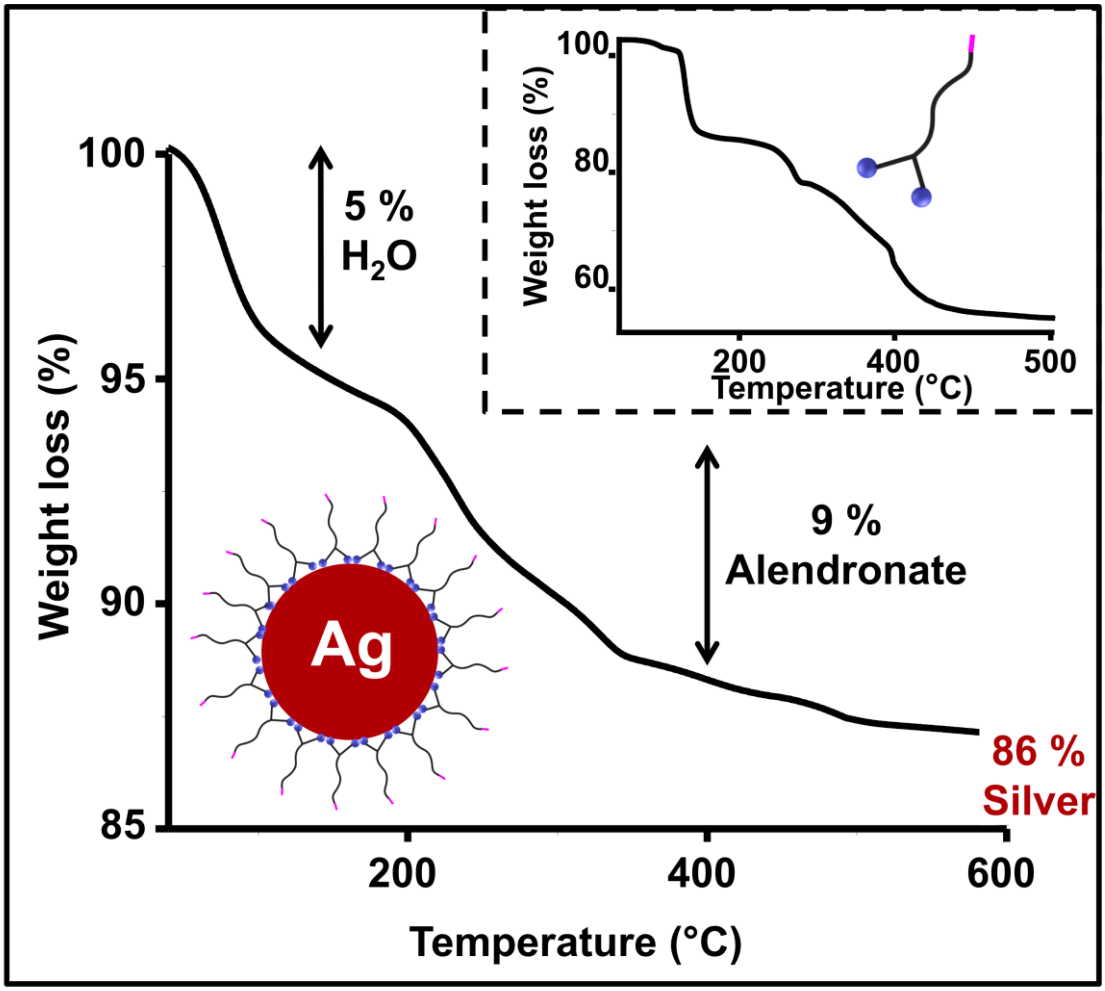

Figure S8. TGA curve of Ald@AgNPs and free alendronate (inset).

The initial sharp decrease in weight (30 °C to 180 °C) corresponds to the removal of physisorbed water molecules. The second major loss (200 °C to 400 °C) corresponds to the removal of the organic layer of alendronate molecules. These data correspond to a composition of 86 % silver and 9 % alendronate.

With the following equation, these percentages can be used to calculate the number of alendronate per NP.

	Weight loss (%)	Mass in 1 g (g)	n in 1 g (mol)	Number of entity in 1 g
AgNPs	85.93	0.86	$n_{Ag}= 7\times10^{-3}$	$^{*}N_{nano}=3.4\times10^{16}$
Alendronate	9.07	0.09	4.0×10^{-4}	2.1×10^{20}

Table S1. TGA calculations for Ald@AgNPs.

$$N_{nano} = \frac{n_{NPs} \times M_{NPs}}{\rho \times \frac{4}{3} \times \pi \times R^3}$$

(*) Where R is NP radius, as obtained from TEM analysis, ρ is NP density, M_{NPs} is molar mass of Ag, and n_{NPs} is the number of moles of NPs as deduced from TGA.[4] An average of 4115 alendronate molecules per nanoparticle was calculated for Ald@AgNPs of 11 nm diameter.

	Weight loss (%)	Mass in 1 g (g)	n in 1 g (mol)	Number of entity in 1 g
Ag	82.14	0.82	$n_{Ag}= 7\times10^{-3}$	$^{*}N_{nano}=3.4\times10^{16}$
Alendronate	5.82	0.06	2.3×10^{-4}	1.4×10^{20}
Dox	2.08	0.02	3.8×10^{-5}	2.3×10^{19}

Table S2. TGA calculations for Dox-Ald@AgNPs.

	Weight loss (%)	Mass in 1 g (g)	n in 1 g (mol)	Number of entity in 1 g
Ag	83.34	0.83	$n_{Ag}= 7\times10^{-3}$	$^{*}N_{nano}=3.4\times10^{16}$
Alendronate	6.00	0.06	2.4×10^{-4}	1.4×10^{20}
Rho	3.32	0.03	6.1×10^{-5}	3.6×10^{19}

Table S3. TGA calculations for Rho-Ald@AgNPs.

2.9. *In vitro* Dox release

For *in vitro* release, solutions of Dox-loaded NPs were stirred at either pH = 7.4 or pH = 5.4. The concentration of drug released from the NPs was determined at different times by Fluorescence spectrophotometry at the Dox specific excitation wavelength of λ_{ex} = 485 nm. The cumulative release (%) was calculated from the following formula:

$$\textbf{Cumulative release} = \frac{C_t}{C_0} \times 100$$

Where C_t is the concentration of Dox at t hours released. C_0 is the total concentration of Dox

3. Biological studies

3.1. Cell lines and culture

HeLa cells were obtained from the American Tissue-Type Culture Collections (ATCC) and cultivated at 37 °C in DMEM containing 10% FBS, 4% glutamine and 1% penicillin/streptomycin.

3.2. *In vitro* cytotoxicity assay

Cell viability was evaluated using the Promega CellTiter-Blue® cell viability assay. This assay uses the indicator dye resazurin to measure the metabolic capacity of cells—an indicator of cell viability. Viable cells retain the ability to reduce resazurin to resorufin, which is highly fluorescent. Nonviable cells rapidly lose metabolic capacity, do not reduce the indicator dye, and thus do not generate a fluorescent signal. HeLa cells were seeded at a density of 1.10^4 cells per well in 96-well flat-bottom plates and incubated in 10% FBS-medium for 24 h. Then, medium was removed and replaced by 10% FBS-medium containing free alendronate, Ald@AgNP or Dox-Ald@AgNPs. After 48 h incubation, cells were washed with phosphate buffered saline (PBS, Amresco Biotechnolgy grade) and incubated with 10 µL of CellTiter-Blue® reagent for an additional 6 h at 37 °C. The fluorescence corresponding to the resorufin (which reflects the relative viable cell number) was measured at 590 nm using a Synergy H1 hybrid reader from Biotek. The measurement was performed on untreated cells as a blank control. This assay allows the determination of the half maximal inhibitory concentration (IC_{50} value), which is a standard measure of a compounds ability to suppress biological or biochemical functions.

Silver nanoparticle coated with a non-toxic coating (starch) were prepared according to the synthesis described by Kahrilas et al.[5] and their toxicity on HeLa cancer cells was tested. After 48 hours of incubation, the cell viability was considerably reduced with an IC50 equal to 27 µM comparing to untreated Hela cells, confirming the toxic effect of AgNPs.

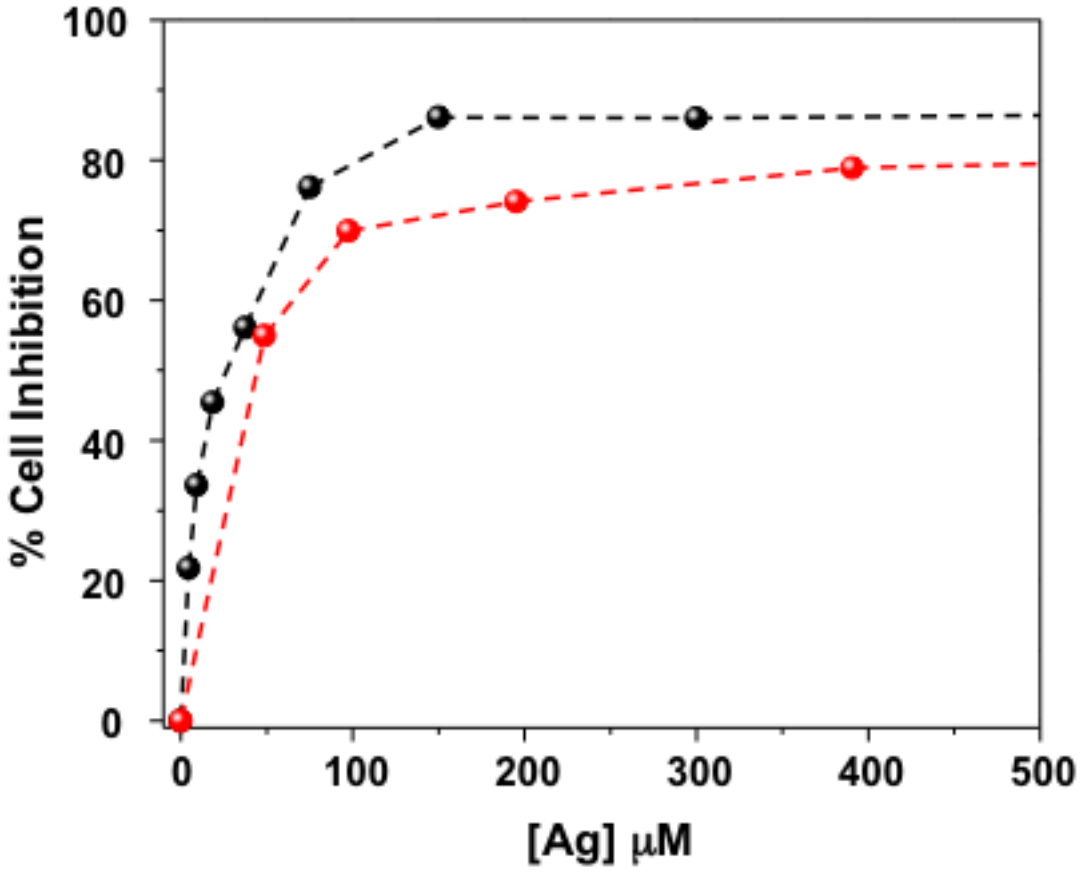

Fig. S9. Inhibition of HeLa cell proliferation after 48 hours as a function of molar concentration of AgNP coated with starch (black line), Ald@AgNPs (red line). The IC_{50} of Starch AgNP is equal to 27 μM whereas it is equal to 45 μM for Ald@AgNPs in silver.

3.3. Kinetic uptake measurements

Hela cells were incubated with RhB-Ald@AgNPs, and cellular uptake of the NPs was quantified by measuring the total amount of fluorescence that accumulated within the cells. For the kinetic uptake measurements, Hela cells were incubated with RhB-Ald@AgNPs and subsequently imaged over several hours with confocal microscopy (Olympus FV1000MPE). For this purpose, three-dimensional confocal stacks were taken with an axial resolution of 0.5 μm, and the images were processed with MATLAB to determine the fluorescence inside the cells. Immediately following addition of the RhB-Ald@AgNPs to the cell medium (t = 0), fluorescence was undetectable because of quenching of the dye. However, once the NPs were internalized, the fluorescence increased with time and reached a plateau after 2h. By using an empirical kinetic model:[42]

$$I = I_{\max} * t^h/(t^h + {t_{1/2}}^h)$$

where I_{max} is the maximum value of fluorescence detected, h the hill slope, and $t_{1/2}$ the half time needed to reach I_{max}, uptake half times are estimated to be 77+/–3 min (h = 1.4) for RhB-Ald@AgNPs. This experiment indicates that net internalization occurs until the intra- and extracellular concentrations of the NPs are equal (Figure S10). Examination of the morphology of the cells showed that the NPs are non-toxic at [Ag] = 0.1 □M.

Cellular uptake was monitored for 4 h after incubation, with a temporal resolution of 10 min for the first minutes and 30 min thereafter. The labeling of the nanoparticles with rhodamine resulted in quenching of rhodamine's fluorescence at neutral pH. Low pH induced release of the rhodamine and recovered fluorescence. We used the nanoparticles with quenched fluorescence to reduce the fluorescence background level outside the cells and to quantify the amount of nanoparticles that released the dye during/after internalization due to pH changes in the cell organelles. To make sure that the observed signal corresponded to the cellular uptake kinetics and not to the dye release kinetics, a control experiment was conducted: the cells were incubated with Rho-Ald@AgNPs, washed with fresh medium after 30 min and subsequently monitored via confocal microscopy.

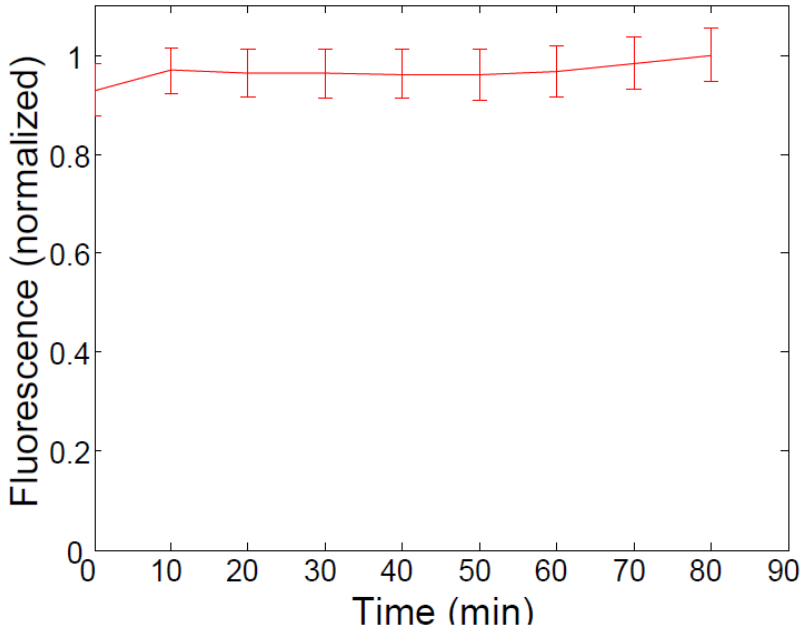

Figure S10. Intracellular fluorescence after 6 h of incubation with Rho-Ald@AgNPs at 4 °C.

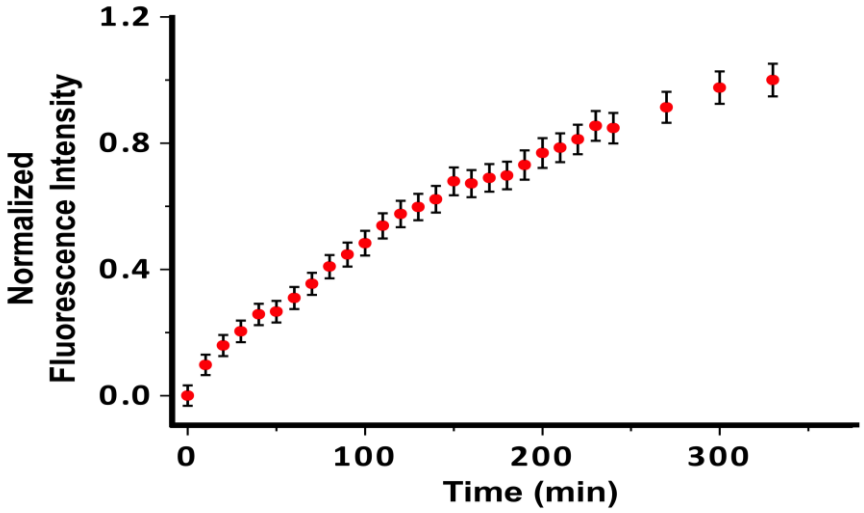

Figure S11. Intracellular fluorescence intensity values plotted against time of RhB-Ald@AgNPs in HeLa cells, as determined by confocal microscopy ([Ag] = 0.1 μM, [RhB] = 2 μM).

3.4 Internalization pathway studies

For these experiments, cells were incubated with endocytic inhibitors 30 min prior to nanoparticle addition. These were incubated for 2 h and then washed with fresh medium before imaging. Table S2 summarizes the concentrations used for the endocytic inhibitors:

Endocytic Inhibitor	Concentration (μ M)
Cloroquine (CQN)	75
Methyl-B-Cyclodextrin (MBCD)	10
Filipin (FLP)	4.6
Cytochalasin (CLN)	20
Chlorpromazine (CPZ)	10

Table S2. Concentration of endocytic inhibitors used in this study.

Cell viability tests were also performed to minimize any experimental artifact that might be due to the cellular condition after drug addition. Figure S12 shows that cell death was negligible for the concentrations used and increased only at 10 fold concentrations.

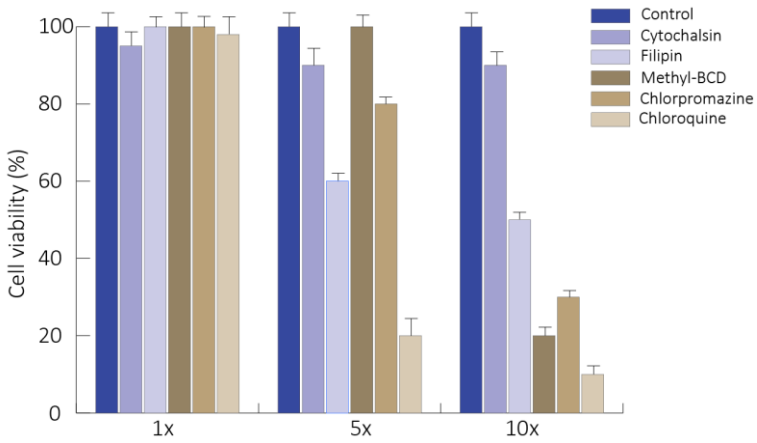

Figure S12. Cell viability tests with cell titer blue.

3.5. Analysis of synergism

Therapies based on synergistic agents allow for reduced drug dosing and toxicity. Two agents act synergistically when their combined effect is greater than the sum of their individual effects. Chou and Talalay derived the combination index (CI) and median effect equation (MEE) in 1984, and have since established precedents for analyzing synergism.[1] The CI is the natural law–based general expression of pharmacologic drug interactions. It is shown to be the simplest possible way for quantifying synergism or antagonism.

The resulting combination index (CI) theorem of Chou-Talalay offers quantitative definition for additive effect (CI = 1), synergism (CI < 1), and antagonism (CI > 1) in drug combinations.

The prerequisite is the dose-effect curves for each drug alone. Each drug not only has a different potency (the Dm value) but also a different shape of the dose-effect curve (the m value). For any determination of synergy, one needs to know both the potency and the shape of the dose-effect curve of each drug.

$$CI = \frac{D_{comb,1}}{D_{alone,1}} + \frac{D_{comb,2}}{D_{alone,2}} + \propto \frac{D_{comb,1}D_{comb,2}}{D_{alone,1}D_{alone,2}}$$

Where CI is combination index; $D_{alone,1}$, dose of drug 1; $D_{alone,2}$, dose of drug 2; $D_{comb,1}$, combination dose of drug 1; $D_{comb,2}$, combination dose of drug 2. For mutually nonexclusive drugs, $\propto = 1$ (independent modes of action of the drugs).

The determination of synergy *in vitro* and in animals follow the same principle that is why we used the values of IC50 measured previously.

$$CI = \frac{IC_{50}\,Ald@AgNPs}{IC_{50}Ald} + \frac{IC_{50}\,Dox\text{-}Ald@AgNPs}{IC_{50}Dox} - \frac{IC_{50}\,Ald@AgNPs \;*\; IC_{50}\,Dox\text{-}Ald@AgNPs}{IC_{50}Ald * IC_{50}Dox}$$

$$CI = \frac{10}{500} + \frac{0.1}{3} - \frac{10 * 0{,}1}{500 * 3}$$

Combination Index = 0.05

In our case the CI value is less than one (0.05), which confirmed the synergistic effect of Ald and Dox delivered using the AgNPs.

4. Optimized geometries obtained with DFT calculations

Ald^-, rTPSSh/ECP28MWB/6-311G(d,p), 0 imaginary frequencies, charge -1, multiplicity 1

Center Number	Atomic Number	Coordinates (Angstroms) X	Y	Z
1	15	-1.038279	1.591050	0.004607
2	8	-2.457673	1.797856	-0.540223
3	8	-1.086989	1.482423	1.645544
4	8	0.016796	2.605836	-0.363070
5	6	-0.580379	-0.176080	-0.395236
6	8	-0.497560	-0.317890	-1.833859
7	1	-0.631727	-1.266514	-1.994704
8	15	-1.969089	-1.275692	0.197638
9	8	-2.121582	-1.020115	1.700688
10	8	-1.700222	-2.677394	-0.309074
11	8	-3.261761	-0.690201	-0.612782
12	6	0.736697	-0.637868	0.259891
13	1	0.680910	-0.448620	1.336128
14	1	0.806548	-1.725776	0.125497
15	6	1.987521	0.021853	-0.330184
16	1	1.998419	-0.154417	-1.410470
17	1	1.927104	1.103910	-0.182856
18	6	3.272689	-0.533800	0.296516
19	1	3.323559	-1.617422	0.137883
20	1	3.264813	-0.361037	1.379078

21	6	4.498261	0.129605	-0.315978
22	1	4.567295	-0.050102	-1.388424
23	1	4.516858	1.203209	-0.131335
24	1	-3.145168	0.311096	-0.641659
25	1	-1.531294	0.618220	1.875736
26	7	5.777514	-0.420318	0.283053
27	1	6.602974	0.029053	-0.120236
28	1	5.808132	-0.269685	1.294413
29	1	5.862686	-1.426435	0.118055

E(RTPSSh) = -1463.6063683 Hartree
Zero-point correction = 0.224542
Thermal correction to Energy = 0.241773
Thermal correction to Enthalpy = 0.242717
Thermal correction to Gibbs Free Energy = 0.179832
Sum of electronic and zero-point Energies = -1463.381827
Sum of electronic and thermal Energies = -1463.364595
Sum of electronic and thermal Enthalpies = -1463.363651
Sum of electronic and thermal Free Energies = -1463.426536

Ald@Ag_2^{2-}, uTPSSh/ECP28MWB/6-311G(d,p), 0 imaginary frequencies, charge -2, multiplicity 3

Center Number	Atomic Number	Coordinates (Angstroms) X	Y	Z
1	47	2.391816	1.297025	0.812485
2	47	2.623843	-0.948276	-1.035755
3	15	-0.547299	0.682774	-1.197973
4	8	0.959685	0.993543	-1.222097
5	8	-1.132583	-0.033388	-2.394694
6	8	-1.325163	2.147073	-1.042428
7	6	-1.059646	-0.077435	0.434958
8	8	-1.075729	1.038429	1.388421
9	1	-0.208798	0.926460	1.846219
10	15	0.176578	-1.329627	1.151255
11	8	0.855471	-2.064261	-0.037929
12	8	-0.590999	-2.265104	2.084885
13	8	1.133743	-0.356224	1.930962
14	6	-2.465256	-0.688483	0.372790
15	1	-2.445304	-1.495762	-0.367619
16	1	-2.648980	-1.155920	1.345814
17	6	-3.613125	0.274105	0.043331
18	1	-3.592807	1.116156	0.743481
19	1	-3.481536	0.684983	-0.961044
20	6	-4.971449	-0.435303	0.135358
21	1	-5.120193	-0.821115	1.150536
22	1	-4.984081	-1.293754	-0.546338
23	6	-6.107271	0.512612	-0.221552
24	1	-6.169865	1.355339	0.466610
25	1	-6.022574	0.888641	-1.240752
26	7	-7.448578	-0.188919	-0.146368

27	1	-8.217248	0.448060	-0.367902
28	1	-7.497565	-0.969718	-0.805578
29	1	-7.619613	-0.565163	0.789482
30	1	-1.321488	2.322304	-0.080154

E(UTPSSh) = -1756.8942912 Hartree
Zero-point correction = 0.213503
Thermal correction to Energy = 0.235486
Thermal correction to Enthalpy = 0.236430
Thermal correction to Gibbs Free Energy = 0.156098
Sum of electronic and zero-point Energies = -1756.680789
Sum of electronic and thermal Energies = -1756.658805
Sum of electronic and thermal Enthalpies = -1756.657861
Sum of electronic and thermal Free Energies = -1756.738193

Ald@Ag_2^-, uTPSSh/ECP28MWB/6-311G(d,p), 0 imaginary frequencies, charge -1, multiplicity 3

Center Number	Atomic Number	Coordinates (Angstroms) X	Y	Z
1	47	-5.423044	-1.195453	-0.331507
2	47	-4.575547	1.544487	0.717669
3	15	4.317245	-1.237596	1.195626
4	8	5.772879	-1.545998	1.482511
5	8	3.411859	-0.771466	2.316401
6	8	3.618041	-2.602719	0.533824
7	6	4.169109	-0.128165	-0.316603
8	8	4.436542	-0.982574	-1.473471
9	1	5.386460	-0.806439	-1.653120
10	15	5.509526	1.178250	-0.342552
11	8	5.698740	1.820862	1.010221
12	8	4.913937	2.345642	-1.376955
13	8	6.642114	0.534004	-1.125786
14	6	2.774901	0.491677	-0.473068
15	1	2.602734	1.151786	0.384105
16	1	2.794593	1.117203	-1.372227
17	6	1.612092	-0.501415	-0.586085
18	1	1.829489	-1.224350	-1.379113
19	1	1.516092	-1.060230	0.347662
20	6	0.294968	0.220056	-0.902845
21	1	0.386614	0.755640	-1.854941
22	1	0.083554	0.965308	-0.127259
23	6	-0.858187	-0.770959	-0.983701
24	1	-0.696093	-1.521197	-1.757861
25	1	-1.030736	-1.273876	-0.032245
26	7	-2.154637	-0.078741	-1.334083
27	1	-2.944988	-0.740180	-1.371267
28	1	-2.416336	0.631448	-0.632663
29	1	-2.098878	0.390933	-2.240799
30	1	3.890137	-2.592221	-0.403121
31	1	4.401835	2.993807	-0.874447

```
 ---------------------------------------------------------------------
 E(UTPSSh) = -1757.3588538 Hartree
 Zero-point correction = 0.224593
 Thermal correction to Energy = 0.247295
 Thermal correction to Enthalpy = 0.248239
 Thermal correction to Gibbs Free Energy = 0.165276
 Sum of electronic and zero-point Energies = -1757.134261
 Sum of electronic and thermal Energies = -1757.111559
 Sum of electronic and thermal Enthalpies = -1757.110615
 Sum of electronic and thermal Free Energies = -1757.193577
```

Ald@Ag^{2-}, uTPSSh/ECP28MWB/6-311G(d,p), 0 imaginary frequencies, charge -2, multiplicity 2

```
 ---------------------------------------------------------------------
 Center     Atomic                   Coordinates (Angstroms)
 Number     Number                X           Y           Z
 ---------------------------------------------------------------------
      1         47             -5.813911    0.050140    0.102984
      2         15              2.870272    1.674165   -0.276383
      3          8              4.293584    2.131889   -0.028464
      4          8              2.238148    1.904952   -1.633321
      5          8              1.884444    2.401756    0.858649
      6          6              2.647379   -0.103324    0.304750
      7          8              2.570232   -0.043707    1.765684
      8          1              3.494296   -0.240102    2.035432
      9         15              4.160906   -1.139754   -0.065130
     10          8              4.670727   -0.920387   -1.469457
     11          8              3.599480   -2.709785    0.029138
     12          8              5.033829   -0.987635    1.170453
     13          6              1.367327   -0.755794   -0.232415
     14          1              1.467453   -0.838076   -1.320770
     15          1              1.326233   -1.774213    0.170118
     16          6              0.053709   -0.037424    0.099791
     17          1             -0.015897    0.100905    1.184751
     18          1              0.061732    0.957268   -0.352699
     19          6             -1.167765   -0.822853   -0.393914
     20          1             -1.167901   -1.827479    0.049709
     21          1             -1.105470   -0.957093   -1.481935
     22          6             -2.487350   -0.126234   -0.049301
     23          1             -2.575567   -0.003999    1.034242
     24          1             -2.514935    0.874245   -0.490279
     25          7             -3.696968   -0.847484   -0.514127
     26          1             -3.676149   -0.932955   -1.529197
     27          1             -3.684029   -1.800885   -0.154488
     28          1              1.979372    1.849335    1.658024
     29          1              3.272415   -2.990196   -0.836474
 ---------------------------------------------------------------------
 E(UTPSSh) = -1610.0177542 Hartree
 Zero-point correction = 0.209555
 Thermal correction to Energy = 0.229619
 Thermal correction to Enthalpy = 0.230563
 Thermal correction to Gibbs Free Energy = 0.156772
 Sum of electronic and zero-point Energies = -1609.808200
 Sum of electronic and thermal Energies = -1609.788135
```

```
Sum of electronic and thermal Enthalpies = -1609.787191
Sum of electronic and thermal Free Energies = -1609.860982
```

5. References

[1] G. R. Kieczykowski, R. B. Jobson, D. G. Melillo, D. F. Reinhold, V. J. Grenda, I. Shinkai, *J. Org. Chem*. **1995**, *60*, 8310.

[2] L. Cervera-Gontard, D. Ozkaya, R. Dunin-Borkowski, *Ultramicroscopy*, **2011**, *111*, 101.

[3] a) Ievlev, D.; Rabin, I.; Schulze, W.; Ertl, G. *Chem. Phys. Lett.,* **2000**, *328*, 142; b) Zheng, J.; Dickson, R. M. *J. Am. Chem. Soc*., **2002**, *124*, 13982; c) Maali, A.; Cardinal, T.; Treguer-Delapierre. *Mona. Physica E.* **2003**, *17*, 559. d) Parkash Siwach, O.; Sen, P. *J. Lumin.,* **2009**, *129*, 6.

[4] S. Verma, D. Pravarthana, *Langmuir*, **2011**, *27*, 13189.

[5] Kahrilas *et al. ACS Sustainable Chem. Eng.,* 2014, **2**, 590−598.